

## Theoretical infrared, Raman, and optical spectra of the $B_{36}N_{36}$ cage

Rajendra R. Zope,<sup>1</sup> Tunna Baruah,<sup>2,3</sup> Mark R. Pederson,<sup>2</sup> and Brett I. Dunlap<sup>4</sup>

<sup>1</sup>*Department of Chemistry, George Washington University, Washington D.C. 20052, USA*

<sup>2</sup>*Code 6392, Center for Computational Materials Science, U.S. Naval Research Laboratory, Washington, D.C. 20375, USA*

<sup>3</sup>*Department of Electrical Engineering and Materials Science Research Center, Howard University, Washington, D.C. 200059, USA*

<sup>4</sup>*Code 6189, Theoretical Chemistry Section, U.S. Naval Research Laboratory, Washington, D.C. 20375, USA*

(Received 24 September 2004; published 17 February 2005)

The  $B_{36}N_{36}$  fullerene-like cage structure was proposed as a candidate structure for the single-shell boron-nitride cages observed in electron-beam irradiation experiment. We have performed all electron density-functional calculations, with large polarized Gaussian basis sets, on the  $B_{36}N_{36}$  cage. We show that the cage is energetically and vibrationally stable. The infrared, Raman, and optical spectra are calculated. The predicted spectra, in combination with experimentally measured spectra, will be useful in conclusive assignment of the proposed  $B_{36}N_{36}$  cage. The vertical and adiabatic ionization potentials as well as static dipole polarizability are also reported.

DOI: 10.1103/PhysRevA.71.025201

PACS number(s): 36.40.-c, 36.90.+f

The discovery of carbon fullerenes [1], the synthesis of boron nitride (BN) nanotubes [2], and the fact that the BN pair is isoelectronic with a pair of carbon atoms, led to the search for fullerene analogues of BN. The carbon fullerenes are made close by introducing 12 pentagons in the hexagonal network of carbon atoms. The exact BN analogues of fullerenes are not preferred as the presence of a pentagonal ring does not permit an alternate sequence of B and N atoms. However, by Euler's theorem, it can be shown that fullerene-like alternate BN cages can be formed using six isolated squares [3,4]. The square contains four BN bonds with alternate boron and nitrogen atoms. Several theoretical works have reported the possible candidate structures for the BN cages [3–10].

On the experimental side, there are also a few reports of synthesis of hollow BN structures [10–14]. In a series of experiments by Oku and co-workers, boron nitride clusters of different sizes were reported [10–12]. Perhaps the most interesting result of these works was the production of  $B_{24}N_{24}$  in abundance. We performed theoretical calculations [8,9] on  $B_{24}N_{24}$ , and think that the roundness of the octahedral  $B_{24}N_{24}$  cluster is the most likely explanation of its unexpected abundance.

In another set of experiments, Stéphan *et al.* irradiated BN powder and BN material [13] and observed small BN cage-like molecules. The irradiated derivatives were either close-packed cages or nested cages. The most observed cages in the experiment had diameters in the size range 4–7 Å; the octahedral  $B_{12}N_{12}$ ,  $B_{16}N_{16}$ , and  $B_{28}N_{28}$  cages were proposed as possible structures. A subsequent tilting experiment in an electron microscope by Goldberg and co-workers permitted viewing of the irradiation-induced BN cages in different directions and corroborated the proposal of octahedral structures for the observed BN cages [14]. From the high-resolution transmission electron microscopy images (HRTEM), they observed single-shelled cages of size 9–10 Å, with rectangle-like outlines. The  $B_{36}N_{36}$  cage has roughly similar dimension and was proposed as a candidate structure by Alexandre *et al.* [15] and Oku *et al.* [10]. Alexandre *et al.* also performed a finite-range pseudopotential

density-functional theory (DFT) calculation on the  $B_{36}N_{36}$  and showed that the  $B_{36}N_{36}$  cage is energetically stable and has a large energy gap between its highest occupied molecular orbital and lowest unoccupied molecular orbital (HOMO-LUMO). These conclusions were subsequently confirmed by all electron calculations using the Slater-Roothan (SR) method [8]. These calculations show that the proposed  $B_{36}N_{36}$  cage has an overall size of about 8 Å, smaller than single-shelled BN cages observed in the experiment. So far, the proposal of  $B_{36}N_{36}$  as the observed structure has not yet been verified in alternative experiments. It is the purpose of the present work to ascertain the stability of proposed cage structure of  $B_{36}N_{36}$  with respect to small distortions and to provide its spectroscopic data—the infrared (ir), Raman, and optical spectra—for comparison with experimental spectra. The comparison of the calculated and experimentally measured spectra has played an important role in structure determination in the past. We hope that the present work will stimulate further experimental works, which, combined with the predicted spectra, would unambiguously confirm the proposal of the  $B_{36}N_{36}$  fullerene-like cage.

Our calculations were carried out at the all-electron level using the NRLMOL suite of codes [16]. The exchange-

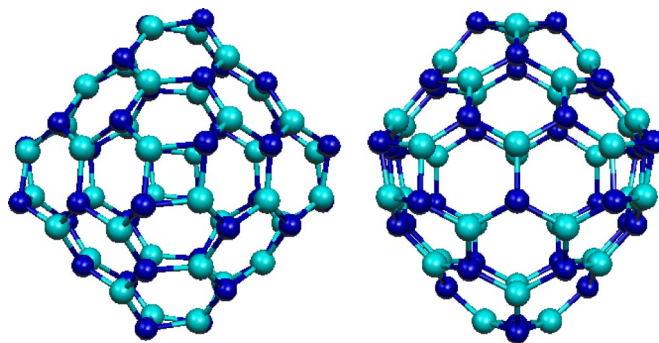


FIG. 1. (Color online) Two different views of optimized  $B_{36}N_{36}$  cages. In the second view, the  $B_{36}N_{36}$  cage is rotated by  $45^\circ$  around a vertical axis passing through the center of the square.

TABLE I. The optimized coordinates of inequivalent atoms in  $B_{36}N_{36}$  in atomic units.

Atom	X	Y	Z
B	-1.340	4.713	4.713
B	-7.771	-1.224	-1.224
B	6.099	2.739	2.739
N	1.457	4.876	4.876
N	8.189	1.504	1.504
N	-6.057	-2.702	-2.702

correlation effects were treated at the level of the generalized gradient approximation using the Perdew-Burke-Ernzerhof scheme (PBE-GGA) [17]. Large polarized Gaussian basis sets [18] optimized for these density-functional calculations are employed. The B-atom basis set consists of five *s*-type, four *p*-type, and three *d*-type orbitals, each of which were constructed from a linear combination of 12 primitive Gaussians. For N atoms, five *s*-type, four *p*-type, and three *d*-type functions comprised of 13 Gaussian are used. The geometry optimization was performed using the limited-memory Broyden-Fletcher-Goldfarb-Shanno scheme until the forces on each atom were less than 0.001 a.u. The self-consistent calculation was iterated until the energy difference of successive iteration was smaller than 0.000 000 1 a.u. The vibrational frequencies were calculated by diagonalizing a dynamical matrix constructed by displacing the atoms by a small amount [19]. The ir and Raman frequencies were determined from the derivative of the dipole moment and the polarizability tensor.

The optimization of the  $B_{36}N_{36}$  cage (see Fig. 1) was started using its optimized geometry obtained by the SR method [8]. The cage has  $T_d$  symmetry and can be generated from six inequivalent atoms, three for boron and three for nitrogen, using symmetry operations. The optimized coordinates of the inequivalent atoms are given in Table I. These coordinates are with respect to the origin at the center of mass. The average spherical radius of the cage, obtained as the mean of distance of each atom from the center of mass, is 3.94 Å. The SR method predicts a cage of 3.76 Å radius [8]. Thus, the cage has roughly a dimension of 8 Å, somewhat smaller than the observed dimensions of the cage structure in the experiment [14]. Part of this discrepancy could be due to the thermal effects, as our calculations are at  $T=0$  K. The cage is energetically stable with respect to isolated atoms and has a binding energy (BE) of 8.43 eV per atom. The SR method gives a binding energy of 7.53 eV/at using the 6-311G\* basis. The present BE is higher than that of  $B_{24}N_{24}$  cages, which have energies of about 8.3 eV [9]. This result agrees with our predictions by the SR method [8]. The trend of larger BN cages being energetically more stable than smaller ones is similar to that observed in the case of carbon fullerenes [20]. The present calculations, in agreement with earlier predictions by lower theories [8,15], show that the  $B_{36}N_{36}$  cage is characterized by a large HOMO-LUMO gap of 5.0 eV. The HOMO level has  $t_2$  symmetry. The vertical ionization potential (VIP) is calculated as the self-consistent energy differences of the cage and its positive ion with the

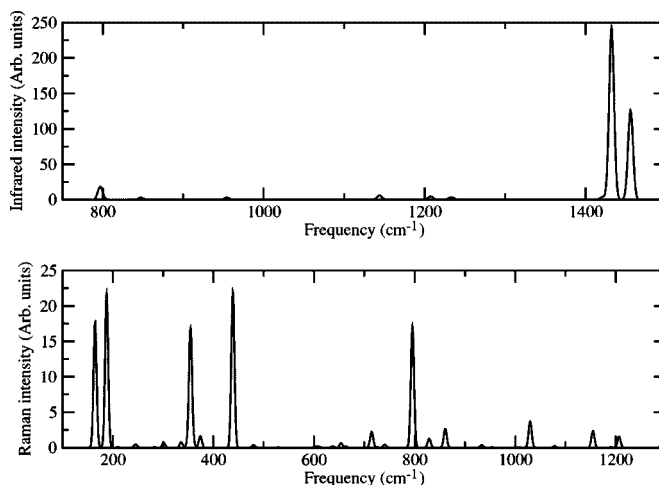


FIG. 2. The infrared (top) and Raman (lower panel) spectrum of  $B_{36}N_{36}$  cage.

same ionic configurations. The calculated VIP is 8.2 eV. This agrees well with 8.4 eV, obtained by the SR method [8]. We have also determined the adiabatic ionization potential from the energy differences of the neutral  $B_{36}N_{36}$  cage and its optimized singly charged cation. The adiabatic ionization potential is 8.1 eV, which is an overestimate as the cation was optimized under symmetry constraint. The mean polarizability of  $B_{36}N_{36}$  calculated from the finite field method is 78 Å<sup>3</sup>. The nuclear frame of  $B_{36}N_{36}$  was assumed to be frozen during the polarizability calculation.

The vibrational analysis within the harmonic approximation indicate that all frequencies are real. Thus, the  $B_{36}N_{36}$  cage is vibrationally stable and corresponds to a minimum on the potential surface. The calculated ir spectrum is presented in Fig. 2. The ir spectrum is broadened by 6 cm<sup>-1</sup>. The ir spectra show two conspicuous peaks at 1432 cm<sup>-1</sup> and 1456 cm<sup>-1</sup>; the intensity of the latter peak (42 D<sup>2</sup>/amu/Å<sup>2</sup>) is half of the former peak. A weak but noticeable absorption (intensity 6 D<sup>2</sup>/amu Å<sup>2</sup>) is found at 797 cm<sup>-1</sup>. All the peaks have  $T_2$  symmetry. The Raman spectrum is also shown in Fig. 2. The Raman spectrum is characterized by multiple peaks in the frequency range 150–900 cm<sup>-1</sup>. Of the two prominent peaks in the low-frequency range, the first one is at 165 cm<sup>-1</sup> and is of  $E$  type. The second one at 188 cm<sup>-1</sup> is due to the triply degenerate mode of  $T_2$  symmetry. All other Raman active frequencies, at 354, 439, 796, 847, and 869 cm<sup>-1</sup>, are of  $A_1$  symmetry. The absorption at 354 cm<sup>-1</sup> corresponds to the symmetric stretching or breathing mode. All vibrational frequencies along with their symmetry type are listed in Table II.

The density of states (DOS) and optical spectra of the  $B_{36}N_{36}$  cluster calculated within DFT are shown in Fig. 3 and Fig. 4, respectively. The HOMO-LUMO gap of this cluster is 5.0 eV. The HOMO has a predominant N character whereas the LUMO is delocalized over the whole cluster. The states near the HOMO and the LUMO have more N character than B character. The HOMO has  $t_2$  symmetry and the LUMO has  $a_1$  symmetry. The HOMO-LUMO transition is weak though symmetry-allowed. The optical spectra show a sharp peak at 5.4 eV which occurs from transitions from

TABLE II. The frequencies, symmetry, ir, and Raman activeness of the vibrational modes.

Frequency (cm <sup>-1</sup> )	Symmetry	ir active	Raman active	Frequency cm <sup>-1</sup>	Symmetry	ir active	Raman active
164	E		√	796	T <sub>2</sub>	√	√
187	T <sub>2</sub>	√	√	806	A <sub>2</sub>		
208	A <sub>1</sub>		√	829	A <sub>1</sub>		√
222	T <sub>1</sub>			847	T <sub>2</sub>	√	√
245	T <sub>2</sub>	√	√	860	A <sub>1</sub>		√
269	T <sub>1</sub>			905	T <sub>1</sub>		
282	E		√	933	E		√
293	T <sub>1</sub>			953	T <sub>2</sub>	√	√
301	T <sub>2</sub>	√	√	966	E		√
335	E		√	967	T <sub>1</sub>		
346	T <sub>2</sub>	√	√	976	A <sub>2</sub>		
354	A <sub>1</sub>		√	979	T <sub>1</sub>		
360	E		√	1006	T <sub>2</sub>	√	√
369	T <sub>1</sub>			1029	A <sub>1</sub>		√
374	T <sub>2</sub>	√	√	1061	T <sub>2</sub>	√	√
419	T <sub>1</sub>			1078	E		√
437	T <sub>2</sub>	√	√	1140	T <sub>1</sub>		
438	E		√	1143	T <sub>2</sub>	√	
462	A <sub>2</sub>			1154	E		√
480	T <sub>2</sub>	√	√	1157	T <sub>2</sub>	√	√
513	T <sub>1</sub>			1159	T <sub>1</sub>		
528	T <sub>2</sub>	√	√	1163	A <sub>2</sub>		
558	T <sub>1</sub>			1166	T <sub>1</sub>		
573	E		√	1175	A <sub>2</sub>		
589	T <sub>2</sub>	√	√	1189	A <sub>1</sub>		√
592	T <sub>1</sub>			1198	T <sub>1</sub>		
605	T <sub>2</sub>	√	√	1206	E		√
612	E		√	1207	T <sub>2</sub>	√	√
636	T <sub>2</sub>	√	√	1232	T <sub>2</sub>	√	√
637	T <sub>1</sub>			1237	T <sub>1</sub>		
640	E		√	1271	T <sub>1</sub>		
653	T <sub>2</sub>	√	√	1288	T <sub>2</sub>	√	√
664	E		√	1299	T <sub>1</sub>		
675	A <sub>1</sub>		√	1304	E		√
677	T <sub>1</sub>			1356	T <sub>1</sub>		
710	T <sub>2</sub>	√	√	1356	T <sub>2</sub>	√	√
714	E		√	1365	E		√
715	A <sub>1</sub>		√	1395	A <sub>1</sub>		√
723	T <sub>1</sub>			1420	T <sub>2</sub>	√	√
726	T <sub>2</sub>	√	√	1432	T <sub>2</sub>	√	√
740	T <sub>2</sub>	√	√	1455	T <sub>2</sub>	√	√
787	T <sub>1</sub>			1456	E		√
792	E		√	1464	A <sub>1</sub>		√
795	A <sub>1</sub>		√				

occupied states within 0.59 eV of HOMO to the unoccupied states within 0.43 eV of LUMO. This peak has contributions from the  $t_2 \rightarrow t_2$  and  $e \rightarrow t_2$  transitions. It also has weak contributions from  $t_2 \rightarrow e$  transitions. There are other higher-energy peaks seen at 9.7 eV and 13.8 eV. The small peak at

9.7 eV arises mainly from a  $t_2 \rightarrow t_2$  transition involving occupied states lying 3.4 eV below the HOMO and unoccupied states 1.3 eV above the LUMO. The broad peak at 13.8 eV is due to a large number of weak transitions involving a large number of low-lying states rather than any sharp strong tran-

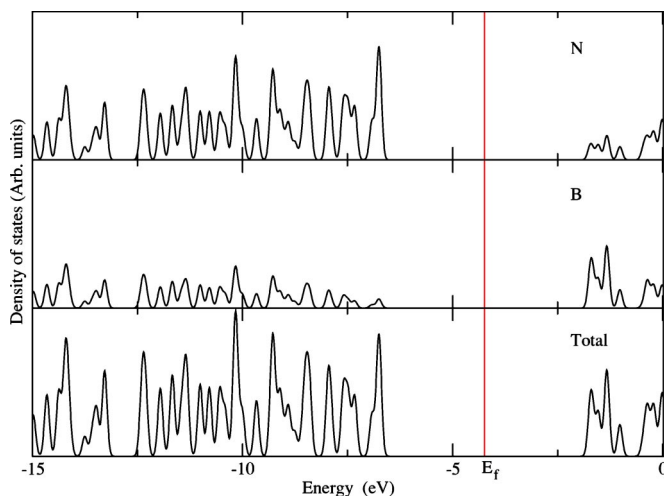


FIG. 3. The total and atom projected density of states of the  $B_{36}N_{36}$  cluster. The position of the Fermi energy is marked by  $E_f$ .

sition. It should be noted that the present calculations are performed within the PBE-GGA at zero temperature and hence the predicted optical spectra will be useful only for qualitative comparison. More accurate spectra can be obtained by the time-dependent DFT or  $GW$  approximation.

In summary, density-functional theory at the level of PBE-GGA is used to examine the vibrational stability of the proposed fullerene-like cage structure of the  $B_{36}N_{36}$  observed in a recent electron-radiation measurement. The cage structure was proposed on the criteria that it satisfied the isolated six square rule for alternate BN cages and has dimension

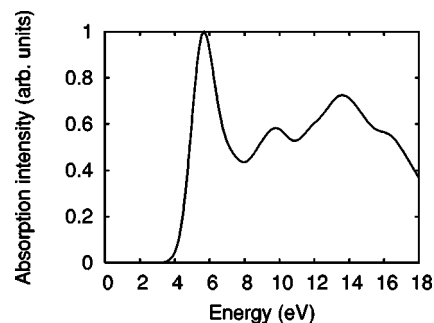


FIG. 4. The optical absorption spectra of  $B_{36}N_{36}$  cluster.

similar to the single-shell BN cages observed in the HRTEM images. The calculations indicate somewhat smaller dimension ( $\sim 8$  Å) of the  $B_{36}N_{36}$  cage than that observed in experiments (9–10 Å). The cage is energetically and vibrationally stable. It has vertical and adiabatic ionization potential of 8.2 and 8 eV, respectively. Its mean static dipole polarizability is  $79$  Å<sup>3</sup>. We have predicted ir, Raman, and optical spectra at the DFT GGA level. We hope that the predicted spectra in this work will stimulate experimental measurements of these spectra. The measured spectra, in combination with the predicted spectra in this work, will play a decisive role in confirmation of the proposed candidate structure.

The Office of Naval Research, directly and through the Naval Research Laboratory, and the Department of Defense's High Performance Computing Modernization Program, through the Common High Performance Computing Software Support Initiative Project MBD-5, supported this work.

- 
- [1] H. W. Kroto, J. R. Heath, S. C. O'Brien, R. F. Curl, and R. E. Smalley, *Nature (London)* **318**, 162 (1985).
- [2] N. G. Chopra, R. J. Luyken, K. Cherrey, V. H. Crespi, M. L. Cohen, S. G. Louie, and A. Zettl, *Science* **269**, 966 (1995).
- [3] M.-L. Sun, Z. Slanina, and S.-L. Lee, *Chem. Phys. Lett.* **233**, 279 (1995).
- [4] H.-Y. Zhu, T. G. Schmalz, and D. J. Klein, *Int. J. Quantum Chem.* **63**, 393 (1997).
- [5] D. L. Strout, *Chem. Phys. Lett.* **95**, 383 (2004), and references therein.
- [6] V. V. Pokropivny, V. V. Skorokhod, G. S. Oleinik, A. V. Kurdyumov, T. S. Bartnitskaya, A. V. Pokropivny, A. G. Sisonyuk, and D. M. Sheichenko, *J. Solid State Chem.* **154**, 214 (2000).
- [7] H. Wu and H. Jiao, *Chem. Phys. Lett.* **386**, 369 (2004).
- [8] R. R. Zope and B. I. Dunlap, *Chem. Phys. Lett.* **386**, 403 (2004).
- [9] R. R. Zope, T. Baruah, M. R. Pederson, and B. I. Dunlap, *Chem. Phys. Lett.* **393**, 300 (2004).
- [10] T. Oku, T. Hirano, M. Kuno, T. Kusunose, K. Nihara, and K. Suanuma, *Mater. Sci. Eng., B* **74**, 206 (2000).
- [11] T. Oku, A. Nishiwaki, I. Narita, and M. Gonda, *Chem. Phys. Lett.* **380**, 620 (2003).
- [12] T. Oku, T. Hirano, M. Kuno, T. Kusunose, K. Nihara, and K. Suanuma, *Mater. Sci. Eng., B* **74**, 206 (2004).
- [13] O. Stephan, Y. Bando, A. Loiseau, F. Willamie, N. Shramchenko, T. Tamiya, and T. Sato, *Appl. Phys. A: Mater. Sci. Process.* **67**, 107 (1998).
- [14] D. Goldberg, Y. Bando, O. Ste'pahan, and K. Kurashima, *Appl. Phys. Lett.* **73**, 2441 (1998).
- [15] S. S. Alexandre, M. S. C. Mazzoni, and H. Chacham, *Appl. Phys. Lett.* **75**, 61 (1999).
- [16] M. R. Pederson and K. A. Jackson, *Phys. Rev. B* **41**, 7453 (1990); **43**, 7312 (1991); K. Jackson and M. R. Pederson, *ibid.* **42**, 3276 (1990).
- [17] J. P. Perdew, K. Burke, and M. Ernzerhof, *Phys. Rev. Lett.* **77**, 3865 (1996).
- [18] D. Porezag and M. R. Pederson, *Phys. Rev. A* **60**, 2840 (1999).
- [19] D. Porezag and M. R. Pederson, *Phys. Rev. B* **54**, 7830 (1996).
- [20] B. I. Dunlap, D. W. Brenner, J. W. Mintmire, R. C. Mowery, and C. T. White, *J. Phys. Chem.* **95**, 8737 (1991).